

1 **Title**

2 A scaffold-free strategy using a PEG-dextran aqueous-two-phase-system (ATPS) for corneal
3 tissue repair

4

5 **Authors:**

6 Lap Tak Hung^{#1}, Stephanie Hiu Ling Poon^{#2}, Wing Huen Yan², Rebecca Lace³, Liangyu
7 Zhou², Jasper Ka Wai Wong², Rachel L Williams³, Kendrick Co Shih², Ho Cheung Shum^{*1},
8 Yau Kei Chan^{*2}

9 # Co-first Authors

10 * Co-corresponding Authors

11

12 **Affiliations:**

13 ¹ Department of Mechanical Engineering, Faculty of Engineering, University of Hong Kong,
14 Rm 7-25, Haking Wong Building, Pokfulam Road, Hong Kong SAR

15 ² Department of Ophthalmology, Li Ka Shing Faculty of Medicine, University of Hong Kong,
16 301B Cyberport 4, 100 Cyberport Road, Pokfulam, Hong Kong SAR

17 ³ Department of Eye and Vision Sciences, Institute of Life Course and Medical Sciences,
18 University of Liverpool, William Henry Duncan Building, 6 West Derby Street, Liverpool, L7
19 8TX

20

21

22 **Correspondence:**

23 Dr. Yau Kei Chan, PhD, Assistant Professor, Department of Ophthalmology, Li Ka Shing
24 Faculty of Medicine, University of Hong Kong, 301B Cyberport 4, 100 Cyberport Road,
25 Pokfulam, Hong Kong SAR, Email: jchanyk@hku.hk.

26 Prof. Anderson Ho Cheung Shum, PhD, Professor and Associate Head, Department of
27 Mechanical Engineering, Faculty of Engineering, University of Hong Kong, Rm 7-25,
28 Haking Wong Building, Pokfulam Road, Hong Kong SAR, Email: ashum@hku.hk.

29

30 **Declaration of interest:**

31 The authors alone are responsible for the content and writing of the paper. This manuscript
32 has not yet been published and is not being simultaneously considered elsewhere for
33 publication.

34

35 **Abstract**

36 Forming thin tissue constructs with minimal extracellular matrix surrounding them is important
37 for tissue engineering applications. Here, we explore and optimize a strategy that enables rapid
38 fabrication of scaffold-free corneal tissue constructs using the liquid-liquid interface of an
39 aqueous-two-phase system (ATPS) that is based on biocompatible polymers dextran and
40 polyethylene glycol (PEG). Intact tissue-like constructs, made of corneal epithelial or
41 endothelial cells, can be formed on the interface between the two liquid phases of ATPS within
42 hours, and subsequently collected simply by removing the liquid phases. The formed corneal
43 cell constructs express essential physiological markers and have preserved viability and
44 proliferative ability *in vitro*. The corneal epithelial cell constructs are also able to re-

45 epithelialize the corneal epithelial wound *in vitro*. The results suggest the promise of our
46 reported strategy in corneal repair.

47

48 Keywords: Tissue engineering; Ophthalmology; Scaffold free; Wound healing; Cornea

49

50 **Introduction**

51 Formation of tissue-like structures with scaffolding materials is now a very common strategy
52 for reconstruction of human tissue, especially those with large-sized defects. The applications
53 include bone, tendon, and neurovascular reconstruction and regeneration procedures.^{1, 2}
54 However, this strategy has fundamental limitations, which hinders its application in forming
55 thin tissues with minimal extracellular matrix, e.g. various cell layers of cornea in the eye.
56 Firstly, scaffolding materials often have suboptimal long-term biocompatibility and
57 biodegradability, hence may trigger activation of adverse immune responses, resulting in post-
58 transplantation complications.³ Moreover, if the degradation rate of scaffolding materials does
59 not match the growth rate of extracellular matrices, the transplanted structures may collapse.
60 In contrast, forming tissue-like structures with a scaffold-free strategy may offer several
61 advantages over scaffold-dependent approaches when forming thin tissues.^{4,5} The preservation
62 of cell-cell junctions and membrane proteins during harvesting of cells from the tissue, may
63 promote construction of tissues for purposes of direct regeneration.⁶ Furthermore, the potential
64 to use a high initial cell density will allow rapid assembly of intact tissue-like structures,
65 thereby eliminating the need for a scaffold.^{7,8} This strategy is useful in forming individual, thin
66 layers of corneal tissue, as these can mimic the anatomical and physiological organisation of
67 both the corneal endothelium and epithelium layers.

68 One notable cause of corneal opacity is corneal endothelial dysfunction,⁹ of which restoration
69 of vision of these patients requires the replacement of the diseased endothelial layer with a
70 healthy endothelial graft.¹⁰ Dysfunction of the endothelial layer leads to corneal edema,
71 whereby the cornea subsequently loses its transparency and resulting in irreversible vision loss.
72 This cell layer does not have the ability to regenerate *in vivo*.^{11, 12} As a result, the replacement
73 of this layer of cells using cadaver donor graft is currently the best approach for treating
74 dysfunctional corneal endothelium.¹³ Unlike *in vivo*, human corneal endothelial cells can

75 proliferate *in vitro* due to absence of contact inhibition.¹⁴ Therefore, corneal endothelial cells
76 can be cultured first and expanded *in vitro*, and subsequently transplanted to the endothelial
77 side of the cornea. However, injecting corneal endothelial cells in the form of a cell suspension
78 is challenging because this approach does not favor large-scale tissue reconstruction.¹⁵
79 Therefore, a planar tissue-like structure of corneal endothelial cells that can be delivered to the
80 eye, as demonstrated in this study, may be of great clinical value, and help overcome cadaver
81 donor grafts limited availability.¹⁶ Meanwhile, other therapeutics are also being developed,
82 which target the corneal endothelium in hopes of preserving or even rescuing the cellular
83 functions of this layer.¹⁷ Another significant etiology of corneal blindness is corneal epithelial
84 injury, resulting from mechanical or chemical insults. Although current strategies for visual
85 rehabilitation depend on full-thickness corneal transplantation (keratoplasty), these can also, in
86 principle, be treated with transplantation of the corneal epithelial layer alone.¹⁸ Corneal
87 epithelium alone also serves as a selectively permeable barrier and maintain ocular surface
88 integrity.¹⁹ Scaffold-based corneal endothelial transplantation is the mainstream for
89 substituting conventional corneal transplantation. However, concerns about cytotoxicity,
90 inflammation, and *in vivo* biodegradability are raised on the use of scaffold materials.²⁰ Another
91 issue would be the anatomical and technical considerations in transplanting a scaffold-based
92 corneal endothelial layer onto the posterior cornea. The presence of the scaffold may interrupt
93 the normal anatomy of the corneal layers since such material is typically not present between
94 the corneal endothelial layer and the Descemet's membrane, where these anatomical layers are
95 supposed to be directly adhered to one another. The presence of the scaffold material could
96 also create a physical barrier between the corneal endothelial cells and the anterior chamber,
97 hence affecting its main function of pumping ions out of the corneal stroma into the anterior
98 chamber.²¹ Another example would be the transplantation of a scaffold-containing retinal
99 pigment epithelial (RPE) layer into the subretinal space. Since such space is surgically created,

100 and is already very small, even with the scaffold material made to be very thin, it would still
101 seem like a relatively thick structure as the retinal is normally already very thin, at around 300
102 μm . This would pose a surgical challenge when inserting the transplanted material into the
103 subretinal space, and more importantly when closing the wound and reattaching the retina since
104 there would be a thick material underneath this layer²². Fabrication of both scaffold-less
105 corneal endothelium and epithelium will aid in our reported strategy of corneal repair. Many
106 established strategies in fabricating tissue-like structure without scaffold are based on
107 magnetic-²³⁻²⁷, electrochemical-^{28, 29} and thermo-responsive techniques^{18, 30-34} in various
108 applications such as heart and liver tissue repair.⁷ However, such methods are currently limited
109 in clinical application owing to the complicated fabrication procedures and high cost.^{35, 36}
110 Moreover, the materials involved in these strategies may affect cellular activities and
111 viability.³⁷⁻³⁹ Hence, there is a justified need for an alternative technique for cell sheet
112 formation.

113 Aqueous-two-phase systems (ATPSs), which consist of two immiscible aqueous phases, have
114 been increasingly adopted as an important tool in biomedical research and applications.^{40, 41}
115 An abundance of biomaterials and their templates can now be fabricated with ease using the
116 liquid-liquid interface formed by ATPS.^{42, 43} In addition, simple scaffold-free tissue structures,
117 such as cell spheroids and cell monolayers, can be formed using such systems.^{44, 45} One
118 particular example is the formation of a robust planar cell construct on the interface of a
119 polyethylene glycol (PEG)/dextran (Dex) ATPS after several hours, via suspension of dermal
120 epithelial cells in the PEG phase of this system.⁴⁶ The interface, which is characterized by
121 interfacial tension between the two aqueous phases, serves as a liquid substrate where cells can
122 be spatially assembled and cell-cell interactions can be formed. The dermal cell constructs
123 formed by this method were able to attach and incorporate into the dermal matrices, as well as
124 undergo differentiation and stratification to form skin-like tissue. Bilayer constructs were also

125 produced via this method, and mechanical strength and cellular physiological markers were
126 demonstrated to be suitable for *in vitro* tissue models. In this study, we explore the strategy of
127 forming scaffold-less cell construct at liquid interfaces. We hypothesise that this method of cell
128 construct formation can be potentially translated to the management of eye conditions, with
129 regards to its transplantation purposes on the ocular surface. After modification and
130 optimization of this technique, we demonstrate that cells isolated from the cornea can be
131 fabricated into robust planar cell constructs *in vitro* comprising mostly of viable cells. The cell
132 constructs can adhere onto anatomical and physiological mimics of corneal surfaces and
133 express physiologically relevant markers *in vitro*. Intact planar cell constructs can be formed
134 within several hours, which is much quicker compared with previously documented methods.
135 Furthermore, the technique does not require any specialized instruments such as electron beam
136 irradiation^{35, 36} for synthesizing thermo-sensitive scaffold, hence can be easily adopted by
137 general biomedical laboratories. Our results demonstrate that formation of planar cell
138 constructs based on all-aqueous liquid systems may act as a versatile strategy for creating
139 corneal-relevant tissue constructs for both ophthalmic clinical use and research purposes.

140

141 **Materials and methods**

142 **Preparation of aqueous two-phase system (ATPS)**

143 The ATPS involved in this work was PEG/Dex. Solutions of PEG (Mw=35,000) (Sigma, USA)
144 and Dex (Mw=500,000) (Pharmacosmos, Demark) were prepared using Dulbecco's Modified
145 Eagle Medium (DMEM, Gibco) or corneal epithelial cell complete growth medium (ATCC)
146 as the solvents. The range of concentrations of PEG and Dex solutions were 2.5 to 15% (w/w)
147 and 5 to 30% (w/w) respectively. To form the biphasic system, the PEG phase was added
148 directly on top of the Dex phase.

149 To pre-equilibrate the ATPS, the two immiscible liquids were mixed and vortexed vigorously.
150 After that, the resulting emulsion was centrifuged at 10,000 x g. for 10 mins to achieve phase
151 separation of PEG-rich and Dex-rich phases. After allowing the phases to settle for 1 day at 4
152 °C, the two immiscible phases, were collected separately for subsequent experiments.

153 The osmolality of solutions of PEG and Dex, with or without equilibration, was measured by
154 freezing point depression osmometer (Model 3320, Advanced Instruments, MA, US) following
155 the manufacturer's instruction. The osmolality of deionized water was calibrated as 0 mOsm/kg.
156 For each sample, the measurement was repeated three times.

157

158 **Culture of eye-related cell sources**

159 The Human Corneal Epithelial cell-Transformed (HCE-T) cell line was kindly provided by Dr.
160 Kaoru Araki-Sasaki from Kansai Medical University.⁴⁷ The cell line was cultured in
161 Dulbecco's Modified Eagle Medium/Nutrient Mixture F-12 (DMEM/F12) supplemented with
162 1% antibiotic-antimycotic and 10% fetal bovine serum. The cell culture reagents were
163 purchased from Gibco, USA.

164 The primary porcine corneal endothelial cells were isolated from porcine eyes, which were
165 obtained from a local wet market within 12 hours post-mortem with reference to previously
166 described methods.⁴⁸ Briefly, the eyes were disinfected with commercially available povidine-
167 iodine solution (Betadine) for 10 minutes at room temperature. The eyeballs were then washed
168 twice with Hank's Balanced Salt Solution (HBSS) supplemented with 100 U/mL Penicillin and
169 100 µg/mL Streptomycin. The anterior segment of the eye was separated, and 2% dispase in
170 Calcium and Magnesium free HBSS was added onto the endothelial side of the cornea. After
171 incubation for 45 minutes in a humidified cell culture incubator, the endothelial side of the
172 cornea was scratched using a metallic cell scraper. HBSS was used to collect the detached

173 corneal endothelial cells from the cornea. The collected cell suspension was filtered using a 70
174 μm cell strainer. The collected endothelial cells, after centrifugation, were cultured in F99 (1:1
175 mixture of Medium 199 and Ham's F-12 Nutrient Mix) supplemented with 10% newborn calf
176 serum, 1% GlutaMAX, 100 U/mL Penicillin, 100 $\mu\text{g}/\text{mL}$ Streptomycin, 0.3 mg/mL chondroitin
177 sulfate and 12.5 $\mu\text{g}/\text{ml}$ endothelial cell growth supplement (ECGS). Unless otherwise specified,
178 all primary corneal endothelial cell culture reagents and supplements were purchased from
179 Gibco, USA. Chondroitin sulfate and ECGS were purchased from Sigma Aldrich, USA.

180 The commercially available primary human corneal epithelial cells (PCS-700-010) were
181 cultured in corneal epithelial cell complete growth medium (ATCC), supplemented with 1%
182 penicillin and streptomycin. Unless otherwise specified, the cell source, as well as all corneal
183 epithelial cell culture reagents and supplements were purchased from ATCC, USA.

184 The culture medium of all the three cell types was changed every 2 days, and the culture was
185 maintained in a humidified incubator at 37°C with 5% CO₂.

186

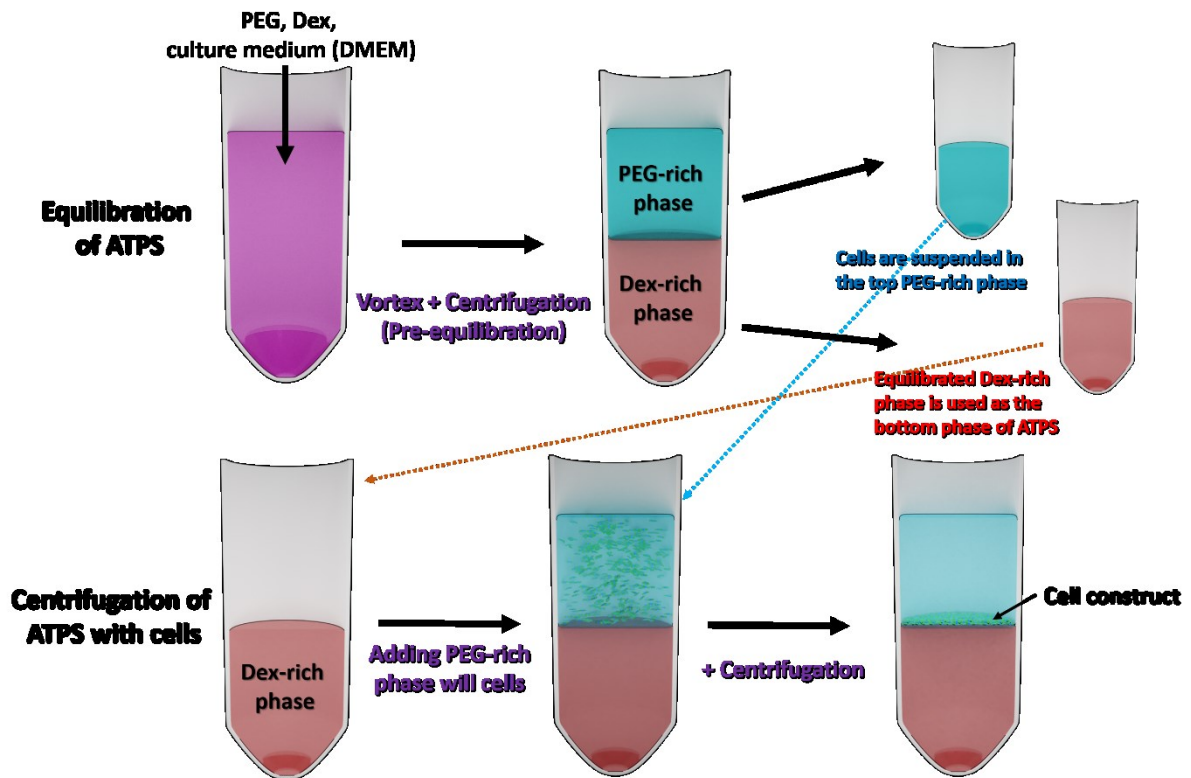
187 **Formation of tissue-like planar constructs**

188 Tissue-like planar constructs were fabricated using pre-equilibrated ATPSs with reference to a
189 previously described method with essential procedural adjustments, as illustrated in Figure 1.⁴⁹
190 Briefly, cells suspended in PEG-rich solution were added to Dex-rich solution in a micro-
191 centrifuge tube. Afterwards, the entire system was centrifuged at 280 x g for 4 mins and
192 incubated in an upright position for 3 hours at 37 °C in 5% CO₂ to allow the self-assembly of
193 the tissue-like planar constructs. The formed cell constructs were harvested by pouring the
194 ATPS solutions out of the microcentrifuge tube into a Petri dish containing HBSS. The cell
195 numbers used to make the tissue-like planar constructs were optimized to be 1 million and 0.2

196 million for corneal endothelial in 600 μ L micro-centrifuge tubes and corneal epithelial cells in
197 200 μ L tubes respectively.

198

199



200

201 **Figure 1** Schematic illustrations of the cell construct formation process

202

203

204 To test the roles of ATPS equilibration and centrifugation on cell construct formation, a non-
205 equilibrated ATPS was formed by preparing PEG and Dex solutions separately without pre-
206 mixing of the two solutions. HCE-T cells were used in this study. Cell construct was formed
207 by adding PEG-cell mixture on top of the Dex phase directly without mixing or vortexing. The
208 entire system was centrifuged at 280 x g for 4 mins and incubated in an upright position for 2
209 hours at 37 °C in 5% CO₂ to allow cell assembly. The cell constructs were harvested as
210 described above.

211

212 **Characterizations of the tissue-like planar constructs of corneal endothelial cells**

213 Uniformity: To investigate the uniformity of the tissue-like planar constructs formed, primary
214 porcine corneal endothelial cells were pre-stained with CellTracker Green CMFDA (Invitrogen,
215 US) before forming the constructs. The harvested tissue-like planar constructs, with green
216 fluorescence signals, was captured using a digital CMOS camera (Hamamatsu, Japan) on a
217 fluorescence microscope (Olympus, Japan). The fluorescence intensity distribution of each
218 constructs was analyzed using an open-source image processing software ImageJ.⁵⁰ Roughness
219 index (RI) was calculated as the percentage standard deviation of the fluorescence intensity
220 distribution from the fluorescence micrograph.

221 Proliferative ability: The endothelial cell constructs were transferred to a conventional cell
222 culture dish and cultured with the abovementioned corresponding culture medium up to 21
223 days. The growth in area of the cell constructs over time was measured using ImageJ. Live-
224 dead assay (L3224, Invitrogen) was used to qualitatively assess the cell viability of the
225 constructs.

226 Physiologically relevant markers: The corneal endothelial cell construct was cultured in
227 conventional plastic culture dish for a month *in vitro* to allow the reconstruction of

228 physiological markers of the corneal endothelium found *in vivo*. Immunocytochemistry was
229 performed to visualize the reconstruction of two physiological markers, namely tight junction
230 protein Zonula occludens-1 (ZO-1) and sodium-potassium ATPase (Na⁺/K⁺ ATPase). After
231 methanol fixation and blocking with 5% normal goat serum, the cell samples were incubated
232 with mouse ZO-1 monoclonal antibody and rabbit ATP1A2 Polyclonal antibody to visualize
233 ZO-1 and Na⁺/K⁺ ATPase respectively. After primary antibody incubation, Alexa Fluor 488
234 conjugated anti-mouse secondary antibody and Alexa 594 conjugated anti-rabbit secondary
235 antibody were incubated with the cell samples, following with DAPI nucleus stain. All
236 antibodies and stains for immunocytochemistry were purchased from Invitrogen, USA. The
237 cell area, which is defined as the area bounded by the tight junction expression, was measured
238 using Adobe Photoshop CC 2020. The cell density was calculated by counting the number of
239 nuclei using ImageJ. Cell suspension seeded with 3000 cells/mm² was performed as a control
240 experiment.

241 Functionality assay: The corneal endothelial cell construct was seeded on a 12-well transwell®
242 permeable membrane (#3460, Corning, USA) pre-coated with Geltrex (Gibco, USA). Single
243 cell suspension with the same cell number as the cell construct was seeded as cell suspension-
244 based transplantation. Empty transwell® was set as control group. The cell culture was
245 maintained for 1 month. Osmolality of both the top and bottom compartment culture media
246 was measured by a freezing point depression osmometer (Model 3320, Advanced Instruments,
247 MA, US) following the manufacturer's instruction. Besides the pump function, the barrier
248 function of the cell was also examined by the same Transwell ® system after 1-month *in vitro*
249 culture. FITC-conjugated Dex (Sigma Aldrich, USA) with a concentration of 1 mg/mL in
250 phenol red-free DMEM (Gibco, USA) was added in the bottom phase and the top chamber was
251 filled with phenol-free DMEM. The Transwell ® system was incubated in humidified incubator
252 for 30 min. After incubation, the medium in the top compartment was collected, and the

253 fluorescence intensity of the medium was measured with multimode microplate reader
254 (Spectramax iD3, Molecular Devices, USA) detected at wavelength of 520 nm with 480 nm
255 excitation light.

256

257 ***Ex vivo* porcine eye model for injection of corneal endothelial cell construct**

258 Fresh porcine eyeball was obtained from a local slaughterhouse within 12 hours post-mortem.
259 Saline was continuously perfused to the anterior chamber of the porcine eye to maintain the
260 chamber not to collapse. Then, two incisions of around 4 mm and 1 mm were created at the
261 limbus region. Corneal endothelial cell construct formed using the proposed ATPS approach
262 was pre-stained with 0.4% Brilliant Blue G and loaded into the intraocular (IOL) injector
263 (UNFOLDER Platinum 1 Series Delivery System, Johnson & Johnson). Brilliant blue G is a
264 widely used dye to stain the donor corneal endothelial graft clinically.^{51, 52} The IOL injector
265 with the cell construct was inserted into the anterior chamber through the 4 mm incision.
266 Similarly, a syringe connected with a cannula was inserted into the anterior chamber of the
267 porcine eye through the 1 mm incision. The cell construct in the IOL injector was then
268 transported into the anterior chamber through the negative pressure applied by the syringe.
269 After the transportation of the cell construct, a sulphur hexafluoride (SF₆) gas bubble was
270 injected into the anterior chamber to push the cell construct onto the endothelial side of the
271 cornea for 10 minutes. After that, the gas bubble was removed.

272

273 **Fabrication of the hydrogel bandage vehicle for delivery of corneal epithelium construct**

274 The hydrogel bandage was fabricated as previously described.⁵³⁻⁵⁵ In brief, poly-ε-lysine
275 (Zhengzhou Bainafo Bioengineering Ltd, China) was cross-linked with nonanedoic acid
276 (azelaic acid) (Sigma-Aldrich), using the activators N-hydroxysuccinimide (NHS) (Sigma-

277 Aldrich) and 1-(3-Dimethylaminopropyl)-3-ethylcarbodiimide HCl (EDCI) (Thermo
278 Scientific) respectively. The solution was then transferred onto a Petri dish and left to
279 polymerize overnight. The gel was subsequently lifted off and sterilized in 70% ethanol for one
280 hour and washed in PBS for 5 times. Circular gels of desired diameters were cut out using an
281 appropriately sized puncher.

282

283 ***In vitro* chemical injury model for testing the transplantation of corneal epithelium**
284 **construct**

285 A monolayer of human corneal epithelial cell was grown on the transwell® permeable
286 membrane pre-coated with 50 µg/mL collagen type I in 0.02M acetic acid. A circular piece of
287 filter paper, soaked in sodium hydroxide (0.1M), was then applied onto the central region of
288 the corneal epithelial layer to create a chemical injury model. Tissue-like epithelial cell
289 constructs were delivered on the *in vitro* chemical wound. Three groups were compared,
290 namely cell construct-only treated group, cell construct transplanted with bandage group, and
291 control group with no cell construct transplantation. The areas of defect remaining on the
292 wounded region were measured over a period of 7 days using ImageJ. In addition, culture
293 medium was extracted from wells each day for analysis of cytokine levels changes over time
294 of healing. These were subsequently run on the LUNARIS™ Human 11-Plex Cytokine Panel
295 by AYOXXA Biosystems GmbH, which covers granulocyte-macrophage colony-stimulating
296 factor (GM-CSF), interferon gamma (IFN-γ), interleukin-1 beta (IL-1b), interleukin-2 (IL-2),
297 interleukin-4 IL-4, interleukin-5 (IL-5), interleukin-6 (IL-6), interleukin-8 (IL-8), interleukin-
298 10 (IL-10), interleukin-12, p70 (IL-12p70), tumor necrosis factor alpha (TNF-α).

299

300 ***Ex vivo* porcine cornea model for testing the transplantation of corneal epithelium**
301 **construct**

302 Primary human corneal epithelial cells were pre-labelled using PKH26 Red Fluorescent Cell
303 Linker Kit (Sigma-Aldrich, US) before forming the constructs. The epithelial cell constructs
304 were transferred to bandage and left to attach overnight at 37 °C in 5% CO₂. The corneal
305 epithelial layer was scraped off using a surgical blade no. 23, including the limbal area. The
306 corneo-scleral button was cut out and a 0.5% agar solution using DMEM solution and agar
307 powder was used to create an agar button to support the shape of the cornea in the 6 well plates.
308 Thereafter, bandages carrying the epithelial cell constructs were applied onto the de-
309 epithelialized *ex-vivo* porcine corneas.

310

311 **Cell construct formation in oil-water system**

312 To highlight the performance of ATPS compared with oil-water system, cell construct was
313 formed using culture medium and fluorinated oil (FC-40) as an oil-water biphasic system. FC-
314 40 was added into a microcentrifuge tube and culture medium mixed with cells were added on
315 top of FC-40. The biphasic system was centrifuged at 1,500 rpm for 4 min and incubated in a
316 humidified incubator at 37°C with 5% CO₂.

317

318 **Statistical analysis**

319 All numeric data obtained were expressed as mean ± standard deviation (S.D.). Data analysis
320 was performed using GraphPad Prism 8. Unpaired *t*-test and one-way ANOVA were performed.
321 A *p*-value less than 0.05 was considered as statistically significant.

322

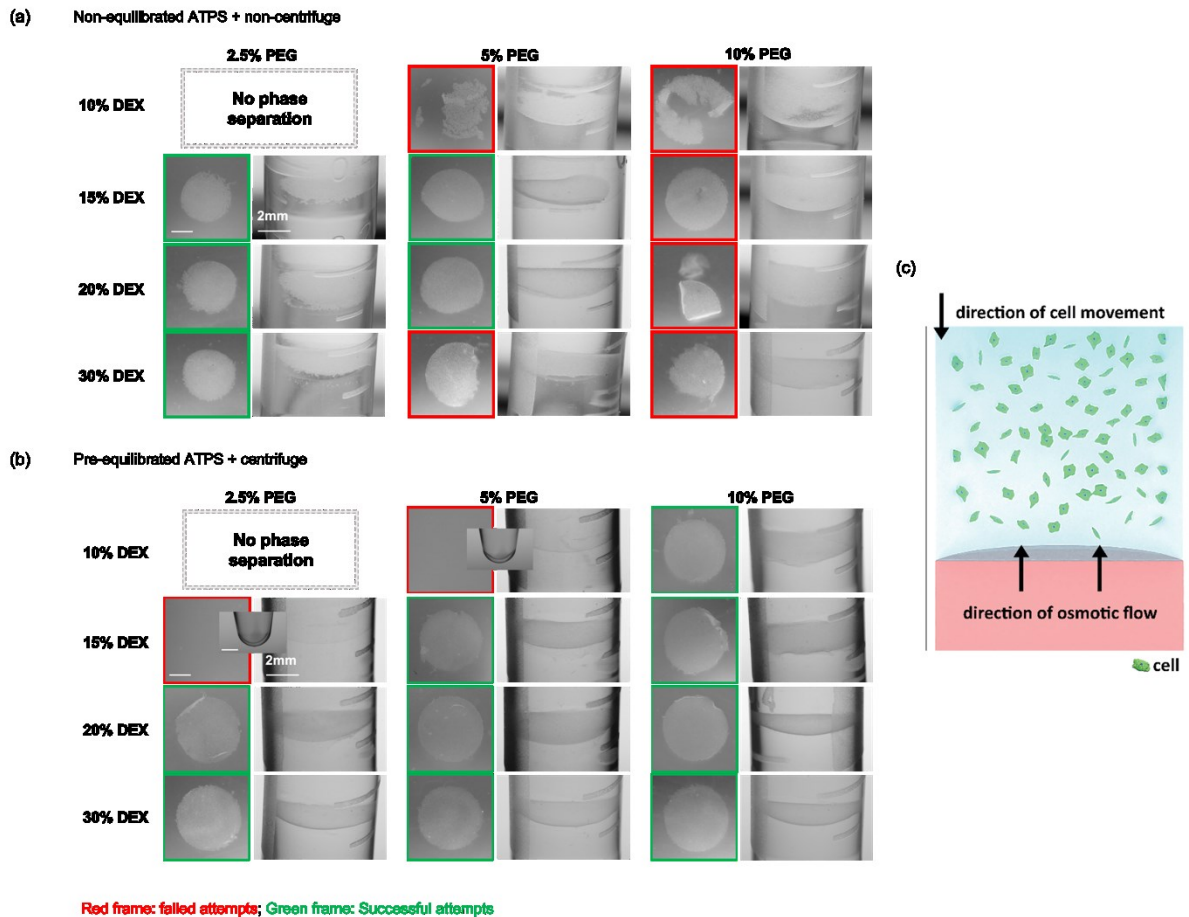
323 **Results and Discussion**

324 The use of the biphasic strategy in forming planar tissue-like constructs in ATPS was first
325 reported in 2015.⁴⁶ Simply by suspending cells in the top PEG-rich phase of the PEG/Dex
326 biphasic system, the cells were able to gather on the PEG/Dex interface and self-assemble to
327 form an intact tissue-like structure within a day. This strategy opens many possibilities for
328 forming transplanted tissue constructs in a simple, rapid, and robust manner. However, the
329 ability of the planar construct to self-assemble is highly dependent on the initial spatial
330 distribution of the cells within the PEG solution. That is, if there is uneven cell distribution in
331 PEG, the cells will subsequently be dispersed across the PEG/Dex interface in a non-uniform
332 manner. Therefore, cell-cell adhesion will be unequal across the tissue construct. Eventually,
333 the final structure may be coarse and bear significant defects; in extreme cases, only fragments
334 may form. These could act as major drawbacks for this promising strategy to be potentially
335 translated to bedside. To overcome these obstacles, we optimize this strategy by adding two
336 new procedures. These are 1) pre-equilibration of the two immiscible liquid phases, and 2)
337 centrifugation of the system after seeding cells in PEG-rich phase. We used HCE-T cells for
338 proof-of-concept during the development of these modifications. Pre-equilibration helped
339 provide a more stable PEG/Dex interface for cells to self-assemble into constructs. The addition
340 of the centrifugation step enabled cells to be more uniformly spaced on PEG/Dex interfaces,
341 hence yielding cell constructs with more homogenous thickness. We also find the time required
342 to form the cell construct can be shortened by these modifications.

343 Above critical concentrations, an aqueous mixture containing two incompatible polymers (e.g.
344 PEG and Dex) will phase-separate.⁴² Via the phase separation phenomenon, concentrated PEG
345 and Dex solutions are prepared separately and are used as two immiscible phases to fabricate
346 tissue-like constructs.⁴⁶ However, since the contents within the two phases are not pre-
347 equilibrated, all molecules within ATPS, including water, PEG and Dex, will move across the

348 interface via diffusion and osmosis. The net movement of molecules makes the liquid-liquid
349 interface unstable and not favorable for the assembly of the tissue-like constructs, as illustrated
350 in Fig. 2c. We hypothesized that reducing the osmotic gradient with the equilibration step is
351 crucial in enhancing the success rate in the formation of an intact tissue-like construct, as the
352 net movement of water molecules can be significantly reduced due to this additional step in
353 our methodology. Therefore, cells can interact and self-assemble into tissue-like constructs on
354 a more stable PEG/Dex interface.⁵⁶ To test our hypothesis, we fabricated the tissue-like
355 constructs with HCE-T cells using ATPSs with different concentration combinations of PEG
356 and Dex, with or without pre-equilibration. To pre-equilibrate the ATPS, the two phases were
357 first vigorously mixed by vortexing, and then centrifuged at a high speed to facilitate phase
358 separation. Our results show that with pre-equilibration together with centrifugation, intact
359 tissue-like constructs can be formed in more ATPSs (with different concentrations of the two
360 polymers), when compared with those without pre-equilibration or centrifugation (increased
361 from 5 to 9 out of 11 ATPSs) (Fig. 2a, b). We further measured the osmolality of the two phases
362 of ATPSs before and after equilibration using a freezing point osmometer. Our results show
363 that the osmolality difference between the two phases can be reduced by 2.73-times to 37.71-
364 times (within various ATPSs) via equilibration of the ATPS (Table 1). This agrees with our
365 hypothesis that pre-equilibration of ATPS is an essential step in forming intact tissue-like
366 constructs.

367



368

369 **Figure 2** The HCE-T cell construct formed using (a) non-equilibrated ATPS without
 370 centrifugation and (b) pre-equilibrated ATPS with centrifugation. Contrast of the photo was
 371 adjusted for better visualization of the cell construct. More successful group is observed in pre-
 372 equilibrated system with centrifugation compared with non-equilibrated system without
 373 centrifugation. Camera photos of the cell construct at the PEG-Dex interface are attached at the
 374 side of the microscopic images. Scale bar = 2 mm. (c) Schematic illustrating the cell construct
 375 formation with osmotic flow.

376

377 Table 1: Osmolality values of PEG and Dex solutions in non-equilibrated and equilibrated
 378 aqueous two-phase systems. Red text indicates non-equilibrated system and green text
 379 indicates equilibrated system. Unit: mOsm/kg. OD: osmolality difference. ($n = 3$, ns not
 380 significant, * $p < 0.05$, ** $p < 0.01$, *** $p < 0.001$, **** $p < 0.0001$, unpaired t -test)

DEX conc.		PEG conc.		
		2.5%	5%	10%
10%	No phase separation	PEG: 390 ± 5	PEG: 505 ± 2	
		Dex: 360 ± 2 (***)	Dex: 360 ± 2 (****)	
		OD: 30	OD: 145	
		PEG: 381 ± 1	PEG: 424 ± 2	
		Dex: 370 ± 1 (***)	Dex: 415 ± 4 (**)	
		OD: 11	OD: 9	
15%		PEG: 357 ± 2	PEG: 390 ± 5	PEG: 505 ± 2
		Dex: 391 ± 6 (***)	Dex: 391 ± 6 (***)	Dex: 391 ± 6 (****)
		OD: 34	OD: 1	OD: 114
		PEG: 373 ± 3	PEG: 392 ± 5	PEG: 453 ± 7
		Dex: 363 ± 5 (*)	Dex: 384 ± 2 (ns)	Dex: 446 ± 7 (ns)
		OD: 97	OD: 8	OD: 7
20%		PEG: 357 ± 2	PEG: 390 ± 5	PEG: 505 ± 2
		Dex: 454 ± 5 (****)	Dex: 454 ± 5 (****)	Dex: 454 ± 5 (****)
		OD: 97	OD: 64	OD: 51
		PEG: 394 ± 5	PEG: 416 ± 2	PEG: 488 ± 5
		Dex: 375 ± 4 (**)	Dex: 407 ± 6 (ns)	Dex: 472 ± 2 (**)
		OD: 19	OD: 9	OD: 27
30%		PEG: 357 ± 2	PEG: 390 ± 5	PEG: 505 ± 2
		Dex: 769 ± 34 (****)	Dex: 769 ± 34 (****)	Dex: 769 ± 34 (***)
		OD: 412	OD: 389	OD: 264
		PEG: 450 ± 2	PEG: 488 ± 4	PEG: 594 ± 6
		Dex: 428 ± 2(****)	Dex: 472 ± 1 (**)	Dex: 601 ± 14 (**)
		OD: 22	OD: 16	OD: 7

381

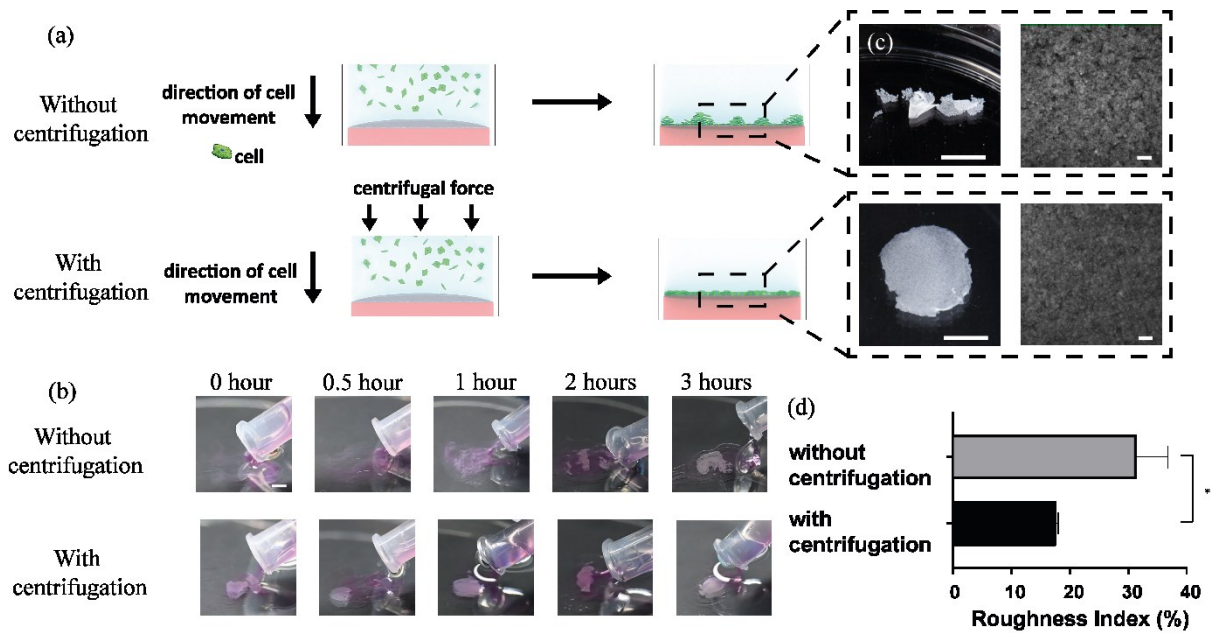
382

383 The self-assembly of the planar construct is affected by the initial spatial distribution of the
384 cells in PEG-rich solution. As the cells are randomly suspended in PEG-rich solution, cells will
385 reach the interface at different times resulting in a cell distribution on the PEG/Dex interface
386 that is unpredictable, leading to highly variable tissue-like constructs. In addition, the thickness
387 of the cell constructs formed will be uneven. To overcome this problem, we hypothesized that
388 centrifuging the whole ATPS after seeding cells in the PEG-rich phase will improve the
389 uniformity of the tissue-like structure formed. Centrifugation is a widely applied technique for
390 assisting the assembly of particles and colloidal structures.⁵⁷⁻⁵⁹ Using centrifugation, all the
391 cells are accelerated to reach and occupy the whole PEG/Dex interface due to the centrifugal
392 force. Hence, this improves the uniformity of the distribution of cells on the interface and
393 speeds up the potential of the formation of cell-cell junctions (Fig. 3a). With the additional
394 centrifugation step, the corneal endothelial cell constructs formed were intact. This is
395 completely different from the fragmented samples that are formed without the centrifugation
396 step (Fig. 3a). From fluorescence intensity measurements, the cell construct formed with
397 centrifugation have a roughness index of 17.70%. This value is significantly lower than that of
398 the cell construct formed without centrifugation (31.46%) (Fig. 3c). Since the fluorescence
399 intensity is related to the tissue thickness, a smaller deviation value indicates a more uniform
400 thickness of the cell construct. We speculate that the low uniformity accounts for the
401 fragmentation of the tissue-like constructs. In the regions of the cell construct that are relatively
402 thinner, the mechanical strength is lower and easily fragmented. With an additional
403 centrifugation step during the fabrication of the cell construct, a more uniform and robust planar
404 tissue-like structure can be formed within ATPS. Moreover, the time for corneal endothelial
405 cell construct formation was shortened with the aid of centrifugation (Fig. 3b). Based on the
406 results obtained after addition of the two procedures, and considering the effect of osmolality
407 to cells,^{60,61} the ATPS components used in the subsequent experiments were chosen to be 10%

408 PEG / 15% Dex. The incubation time for self-assembly of cells was optimized as 3 hours to
 409 minimize the osmolality effect on the cells.

410

411



412

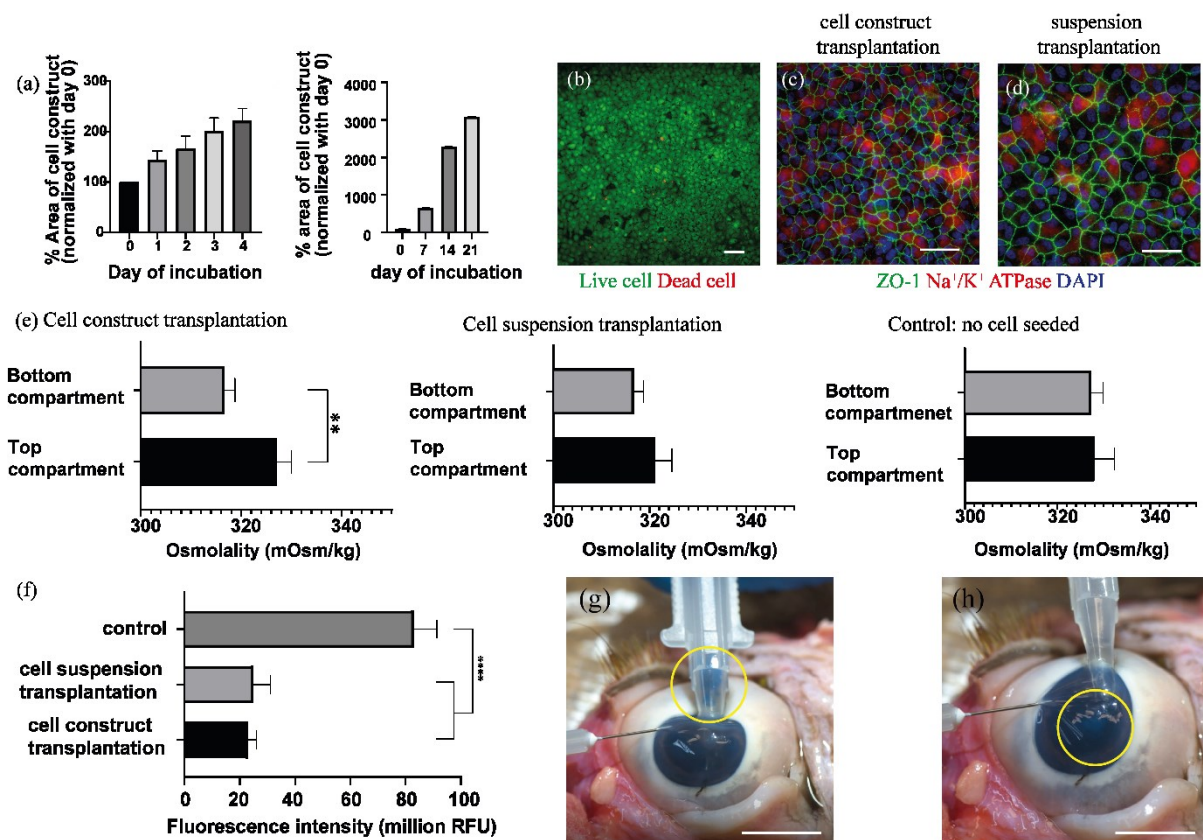
413 **Figure 3** (a) Schematic illustrating the role of centrifugation on cell construct formation. (b)
 414 Comparison of the primary porcine corneal endothelial cell construct formation time by the
 415 approaches with and without centrifugation. The time indicates the incubation time after
 416 construct formation. Scale bar = 3 mm. (c) The camera image (left) and fluorescence
 417 micrograph (right) of the primary porcine corneal endothelial cell construct formed with and
 418 without centrifugation approach respectively. Scale bars = 3 mm for camera image and 100 μ m
 419 for fluorescence micrograph. (d) The roughness index of the pre-stained cell construct formed
 420 with and without applying centrifugation. ($n=3$, $*p < 0.05$, unpaired t -test)

421

422

423 The above shows that the ATPS liquid substrate allows for scaffold-free assembly of cell-based
424 constructs, whereas the additional centrifugation procedure improves the compactness and
425 uniformity of the cell constructs formed.. Using the modified and optimized conditions as
426 aforementioned, we fabricated the planar construct using primary porcine corneal endothelial
427 cells. The primary cells obtained are cautiously cultured with appropriate characterizations
428 prior to use. (Supplementary Fig. 1) The majority of the cells in the cell construct were viable,
429 and these are stained in green using live-dead staining (Fig. 4b). In *in vitro* culture, the area of
430 the cell construct doubles after around 3 days, showing the proliferative capacity of the cells in
431 the construct. Moreover, the cultured cell construct expanded to fill up most of the culture space
432 in 6-well plate after 21-day *in vitro* culture (Fig. 4a). The proliferative ability is important
433 because the corneal endothelial cells need to grow and fully cover the endothelial surface of
434 the cornea after removal of the damaged and diseased cells. The coverage of the corneal
435 endothelial cells on the inner corneal surface is critical for restoration of its function, which is
436 to regulate the water content of the corneal tissue effectively. In addition, the cell constructs
437 cultured *in vitro* can express the physiological markers of corneal endothelial cells that express
438 *in vivo*. The cells expressed high levels of both ZO-1 and Na⁺/K⁺ ATPase, as shown in green
439 and red respectively (Fig. 4c). The reconstruction of these physiological markers is critical in
440 restoring functions of the corneal endothelium. Tight junctions are responsible for resisting the
441 passive diffusion of water,⁶² whereas sodium potassium ATPase regulates the water potential
442 of the corneal tissue.⁶³ These functions are crucial for maintaining the transparency of cornea.
443 Moreover, the endothelial layer formed using the biphasic construct approach has a more
444 compact organization of the cells, when compared with the conventional 2D cell culture
445 method. (Fig. 4c and 4d) The mean cell area of the cells in the planar construct, defined as the
446 area bounded by the ZO-1 expression, is 186.04 μm^2 , which is just 40% of that of cells in 2D
447 cell culture (462.14 μm^2) (Table 2). In converting the mean cell area into cell density, a smaller

448 mean cell area indicates a higher cell density. Since the corneal endothelial cell density is
449 expected to decrease gradually after transplantation, a high initial cell density in the donor graft
450 is more favourable for transplantation purposes.⁶⁴ The higher initial cell density also provides
451 promising evidence for restoration of the corneal function in a more physiological
452 representative manner *in vitro*. To prove that the cell construct is physiologically active *in vitro*,
453 a transwell® system is applied to split the *in vitro* environment into top and bottom components.
454 Since corneal endothelial cells are responsible to pump out excess water from the corneal tissue,
455 the corneal endothelial cells cultured *in vitro* can therefore generate an osmotic gradient
456 between the top and bottom phase if the cultured corneal endothelial cells are physiologically
457 active. As shown in figure 4e, after one-month *in vitro* culture, the cell construct can generate
458 a significantly different osmolality value between the top and bottom compartments in the
459 transwell® system. ($p < 0.01$, unpaired *t*-test, $n=3$). Besides the water transportation, the cell
460 construct was also able to perform the barrier function. From the FITC-Dex diffusion assay
461 (figure 4f), the cell construct transplantation group and cell suspension cultured for 1 month *in*
462 *vitro* were able to resist the FITC-Dex diffusion compared with blank control, hence indicating
463 we were able to reconstruct its physiological functionality. To demonstrate the possibility of
464 the transplantation of the corneal endothelium construct, we perform a trial to transport the
465 construct into an *ex vivo* porcine eye model with reference to a procedure called Descemet
466 Membrane Endothelial Keratoplasty (DMEK). DMEK is a well-established ophthalmic
467 surgical procedure in which a corneal endothelial donor graft is transplanted onto the
468 recipient's eye.⁶⁵ In this trial, the corneal endothelial construct stained with 0.4% brilliant blue
469 G is loaded into the IOL injector. Then, the injector is inserted into the anterior chamber of the
470 porcine eye through an incision, through which the cell construct can be transported into the
471 eye, (Figure 4g). The success of this trial suggests that the ATPS approach in fabricating
472 corneal endothelial construct possesses the translational potential into clinical application.



474

475 **Figure 4** (a) The primary porcine corneal endothelial cell construct is able to proliferate *in*
 476 *vitro*. (b) Majority of the live cells are observed in the cell construct cultured *in vitro* for 4 days.
 477 Green and red expressions are representing live cells and dead cells respectively. Scale bar =
 478 100 μ m. The primary porcine corneal endothelial cell construct can express proteins that are
 479 related to its physiological function *in vitro*. Sodium-potassium ATPase (Na⁺/K⁺ ATPase) and
 480 Zonula occludens-1 (ZO-1), which is stained in red and green respectively, are both expressed
 481 in (c) cell construct transplantation and (d) cell suspension-based transplantation after 1-month
 482 *in vitro* culture. Scale bar = 50 μ m. *ex vivo* injection of the primary porcine corneal endothelial
 483 cell construct into isolated porcine eyeball. (e) The osmolality value of the top and bottom
 484 phases of the transwell® system cultured with cell construct and cell seeded as single cell
 485 suspension. (** $p < 0.01$, unpaired *t*-test, $n=3$) (f) The fluorescence intensity of the top
 486 compartment medium in the Transwell® system cultured with cell construct and cell seeded as
 487 single cell suspension in FITC-Dex diffusion functionality assay. (**** $p < 0.0001$, one-way
 488 ANOVA) (g) The cell construct pre-stained with 0.4% Brilliant Blue G is loaded into an
 489 intraocular injector. The nozzle inserted in the eyeball is connected to the saline perfusion
 490 system. (h) After injection, the cell construct is injected into the anterior chamber of the porcine
 491 eyeball. Scale bar = 1 cm.

492

493 Table 2: Mean cell area and cell density for primary porcine corneal endothelial cell construct

	Mean cell area (μm^2)	p-value with respect to cell construct	Translated cell density (cells/ mm^2)
Cell construct	186.04 \pm 76.62	/	5375.19
Experimental control seeded as cell suspension	462.14 \pm 169.25	< 0.0001 (****)	2163.57

494

495 Besides reconstruction of corneal endothelium, regeneration of corneal epithelium also has a
496 high clinical value.^{18,66} Under corneal epithelial injury, the loss of the epithelial layer can lead
497 to corneal ulcer, as the inner structure of cornea is exposed. Stromal complications such as
498 scarring, hazing, edema, and blindness as an end-stage sequelae may therefore occur.⁶⁷ First-
499 line treatment options for corneal epithelial defects, including drugs, bandage contact lens, and
500 amniotic membrane or corneal donor graft transplantation for severe defects, are available.⁶⁸
501 However, most come with complications and may compromise the long-term efficacy of the
502 respective management strategies.⁶⁹ We believe the rapid formation of corneal epithelial layer
503 through this biphasic strategy may provide an alternative treatment for corneal epithelial
504 defects. To demonstrate such translational potential, we have developed an *in vitro* chemical
505 corneal injury model on a typical transwell® culture system. A monolayer of human corneal
506 epithelial cell is firstly grown on the transwell® permeable membrane. Sodium hydroxide
507 solution, as absorbed by a filter paper, is then applied onto the central region of the corneal
508 epithelial layer to create a chemical injury. Tissue-like corneal epithelial cell constructs are
509 successfully fabricated using the biphasic strategy, and delivered onto the *in vitro* chemical
510 wound. Proliferation of cells from both the cell construct and the edges of the chemical wound
511 is observed from time-lapse images. The percentage areas of defect of the chemical wound,
512 after transplantation of epithelial cell construct, significantly decrease over time. A complete
513 recovery, defined as when the cells re-epithelize to fully cover the wounded area, is achieved
514 after day 7 on the *in vitro* chemical injury model (Fig. 5a). As the epithelial cell construct is
515 not monolayered, the cells which are not adhered to the membrane eventually detach from the
516 cell construct on day 4 (Fig 5b). An intact layer of epithelial cells remains underneath to cover
517 the wound area. The layer successful integrates with the peripheral cells on the transwell®
518 membrane after chemical injury and closes the wound eventually on Day 4. Cytokine studies
519 reveals significant changes in levels in GM-CSF, IL-1b, IL-6, IL-8, and TNF- α . A rise in these

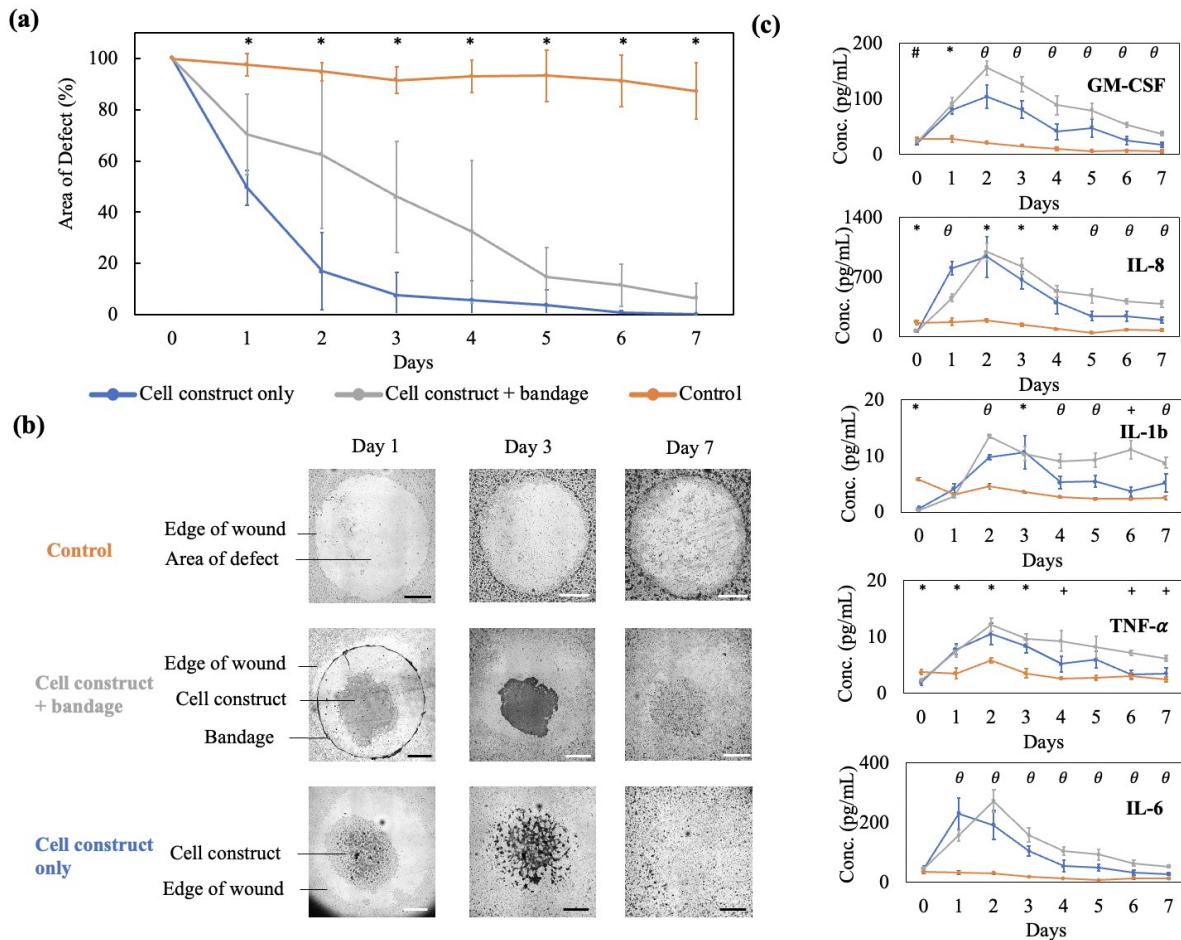
520 levels is observed during the initial period of cell construct transplantation in both the cell
521 construct-only group and the group with cell construct transplantation using the bandage,
522 compared with control group ($p < 0.05$) (Fig 5c). Levels peak generally at either day 2 to 3 for
523 the cytokines, and gradually diminish to reach baseline level by day 7, matching that of control
524 groups. The initial surge in cytokines during day 1 to 3 correlates with an increased rate of
525 proliferation of the cell construct during the same period, hence a greater initial drop in
526 percentage area of defect on the Transwell® chemical injury model. This is expected since
527 GM-CSF, IL-1, IL-6, TNF- α are recognised for aiding corneal epithelial cell migration after
528 injury.⁷⁰ GM-CSF has been demonstrated to improve the rate of corneal epithelial wound repair
529 by increased cell migration both *in vitro* and *in vivo*, but without significant effect on corneal
530 epithelial cell proliferation.⁷¹ IL-1 has been postulated to have additive effect on corneal wound
531 closure with epidermal growth factor (EGF), via increasing the receptor binding ability of EGF
532 up to 110%.^{72,73} It is also believed that IL-1 could induce keratocyte apoptosis, hence regulating
533 the epithelial-stromal interactions by maintaining tissue organisation hence plays a role in
534 corneal wound healing.⁷⁴ In previous studies, elevated TNF- α levels was found after corneal
535 chemical injury, since it is a major proinflammatory cytokine.⁷⁵ Its interaction with other
536 cytokines such as TGF- β and IL-1 β may play a role in balancing of signalling pathways in
537 corneal wound healing.^{75,76} IL-6, on the other hand, is involved in the initial phases of epithelial
538 wound closure by stimulating the epithelial cells.^{77,78} Lastly, IL-8 is positively regulated by
539 macrophage colony-stimulating factors (M-CSF) during active inflammatory processes, as in
540 the chemical insult demonstrated in this *in vitro* model.⁷⁹

541 Since the corneal epithelial cell construct will ultimately be transplanted onto the corneal
542 wound to facilitate repair of the epithelial defect, a hydrogel bandage is needed to act as a
543 vehicle to transport and stabilize the construct on the wound. The bandage will also be able to
544 protect the cell construct from detaching off of the ocular surface after transplantation onto real

545 patients, since it will act as a barrier between friction generation from the ocular surface and
546 the eyelids during blinking action. The corneal epithelial construct can attach well on our
547 antimicrobial peptide hydrogel bandage.⁵³ On the *in vitro* corneal injury model, the corneal
548 epithelial construct on the bandage exhibits similar proliferative capacity to the construct
549 without the bandage vehicle (Fig. 5a and Fig. 5b). The results suggest that the vehicle does not
550 hinder the proliferation of the cells on the wound, and therefore does not affect the potential
551 wound healing capacity of the construct. To further demonstrate its clinical translation potential,
552 the corneal epithelial construct on the bandage is first transported onto a de-epithelialized *ex*
553 *vivo* porcine cornea. The bandage is removed 3 days after transplantation, and the cell construct
554 is successfully retained and attached onto the denuded porcine cornea. (Fig. 6a) Only a small
555 amount of corneal epithelial cells remains on the bandage. The area covered by corneal
556 epithelial cells increases from $14.8 \pm 3.5 \text{ mm}^2$ on day 3 to $18.9 \pm 3.4 \text{ mm}^2$ on day 7 ($n = 6$) (Fig.
557 6a). In comparison the conventional cell-seeding, which involves seeding of corneal epithelial
558 cells onto the bandage directly, allowing them to adhere on the hydrogel surface, then gently
559 placing them onto the denuded corneal surface with cell-side facing down, we observe a
560 reduced transfer of cells from the bandage onto the porcine cornea, with increased retention of
561 cells on the bandage material (Fig. 6b). A thinner layer of epithelial cells is also observed in
562 the conventional cell-seeding group through H&E-stained corneal tissue sections, when
563 compared with ATPS-construct group (Fig. 6c). These results highlight the higher cell
564 transferal efficiency with the ATPS-construct approach for delivering cells onto the corneal
565 epithelial wound. In addition, the multi-layered nature of the epithelium, as demonstrated by
566 the ATPS-construct group, bears greater resemblance to the normal architecture of the corneal
567 epithelium when compared with the transplanted epithelium derived from the conventional
568 cell-seeding group. This is important since the epithelial layer has to be thick enough to act as

569 a protective barrier for the eye, and also thin and hence transparent enough to allow light to
 570 reach the retina.

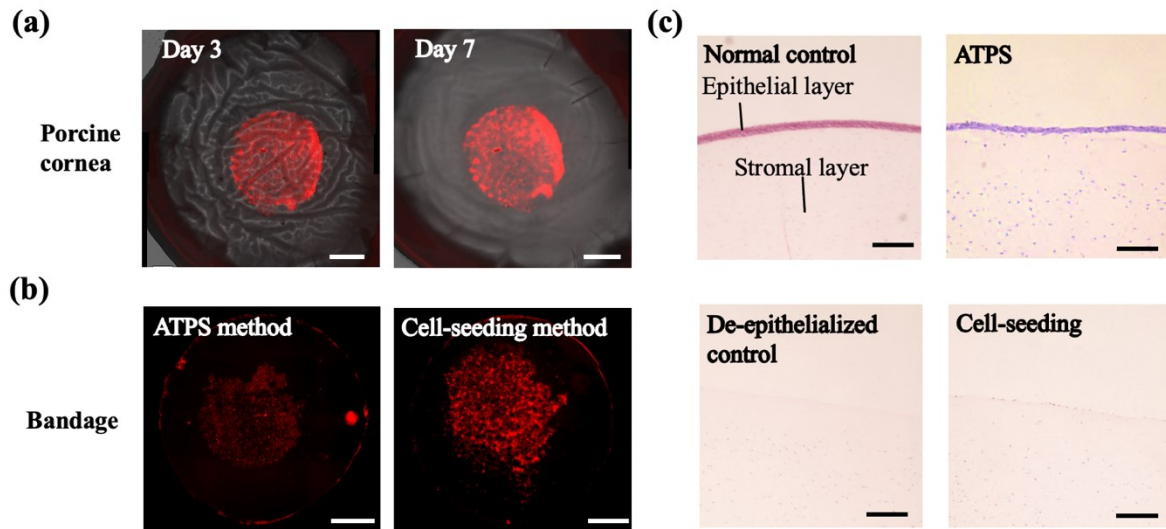
571



572

573 **Figure 5** Results of experiments on the *in vitro* Transwell® chemical injury model. (a) The
 574 area of defect measured in percentage of initial area of injury on the *in vitro* Transwell®
 575 chemical injury model. (b) Wound and cell construct proliferation observed under light
 576 microscopy. Control group demonstrated minimal proliferation of wound edges up until Day 7
 577 post-transplantation. Cell construct proliferation was demonstrable in both cell sheet only
 578 group and cell construct with bandage groups, but the former had much more significant growth
 579 rates. Scale bar = 2 mm. (c) Changes in concentrations of cytokines with cell construct growth
 580 across a 7-day observation period. (* $p < 0.005$ for both cell construct only vs control, and cell
 581 construct with bandage vs control; # $p < 0.005$ only for cell construct vs control; + $p < 0.005$
 582 only for cell construct with bandage vs control; θ $p < 0.005$ for all of cell construct only vs
 583 control, cell construct with bandage vs control, and cell construct vs cell construct with bandage)

584



585

586 **Figure 6** Results of experiments on the *ex vivo* porcine cornea model. (a) Cell construct (in red)
 587 on porcine cornea observed microscopically on Day 3 and Day 7 after removal of bandage.
 588 Scale bar = 2 mm. (b) Remaining cells (in red) adhered on bandage after its removal from
 589 porcine cornea at Day 3, whilst the rest of the cells are transferred onto the porcine cornea
 590 model. Bandage from both ATPS method and cell-seeding method are demonstrated. Scale bar
 591 = 2 mm. (c) H&E staining of corneal sections which underwent cell construct transplantation
 592 via ATPS and conventional cell-seeding method, compared with normal and de-epithelialized
 593 controls Scale bar = 200 μ m.

594

595

596 The use of a liquid-liquid interface as a liquid substrate allows individual cells to gather and
597 assemble to form scaffold-free tissue-like constructs. However, only polymer-polymer ATPS,
598 not other biphasic systems, such as oil-water and oil-oil system, can be used. FC-40, a
599 fluorinated oil, is regarded as a relatively biocompatible oil. We repeated the same experiment
600 using a FC-40/culture medium biphasic system. However, unlike in a PEG/Dex system, the
601 cell constructs could not be formed in FC-40/culture medium system (Supplementary Figure
602 2). Although the oil-water system is extensively used in the fabrication of emulsion-based
603 biomaterials,^{80, 81} the oil phase can lead to protein denaturation and lipid oxidation at the oil-
604 water interface.^{82, 83} We also find that cell construct cannot be formed in polymer-salt ATPS
605 (Supplementary Figure 3). We repeated the cell construct formation experiment with
606 PEG/sodium citrate polymer-salt ATPS and no cell construct formation is observed. The reason
607 could be due to the loss in cell viability in hypertonic environment. Since a significant high salt
608 concentration (at least 5 wt%) is required to establish a salt-polymer ATPS⁸⁴, such high salt
609 concentration environment is undoubtedly not favourable for biological cells. The results
610 highlight the superiority in using polymer-polymer ATPS to form scaffold-less tissue-like
611 constructs using the biphasic strategy. We anticipate this approach to be extended to the
612 fabrication of transplantable cell layers in other areas of the eye, including the retinal pigment
613 epithelium,^{25, 31, 85} which is associated with aged-related macular degradation.^{86, 87} Moreover,
614 the proposed strategy should, in principle, allow layer-by-layer assembly of different cell types.
615 Such assembly can be achieved simply by adding another layer of PEG-cell mixture after
616 forming the first tissue layer.⁴⁶ This strategy may therefore pave the way towards the
617 reconstruction of complex multicellular tissues such as the retina.

618

619

620

621 **Conclusion**

622 The described ATPS interfacial strategy for fabricating corneal-relevant tissue constructs
623 entails modification of the previously described protocol, yet with demonstrable improved
624 success rates and robustness of formed tissue-like constructs. This strategy can be easily
625 implemented in general biomedical laboratories, as no specialized instruments are required.
626 The corneal endothelial cell construct fabricated using this strategy demonstrated proliferative
627 capacity and expression of physiologically relevant markers *in vitro*. The corneal endothelial
628 cell construct could also be able to implant into the anterior chamber of *ex vivo* porcine eyeball
629 using standard surgical tools. Similarly, the corneal epithelial construct expressed its potential
630 to facilitate corneal wound healing *in vitro*. These results demonstrate that formation of planar
631 cell constructs based on all-aqueous liquid systems may act as a versatile strategy for creating
632 corneal-relevant tissue constructs for both potential transplantation purposes.

633

634

635 **Supporting Information**

636 Additional details of experiments including images of experimental results.

637

638 **Figure SI-S1.** Characterization of the isolated porcine corneal endothelial cell. The porcine
639 corneal endothelial cell isolated is physiologically representative with high purity.
640 Physiological markers are expressed after *in vitro* culture. Immunocytochemistry is
641 performed after 1-month culture of the corneal endothelial cells. Green and red expressions
642 are representing Zonula occludens-1 (ZO-1) and N-cadherin (N-cad) expression respectively.
643 Scale bar = 100 μ m.

644 **Figure SI-S2.** Formation of intact cell construct in ATPS but not oil-water systems. (a) Cell
645 construct is formed in ATPS. Black arrow indicates the position of the cell construct. (b) The
646 cell construct formed is intact. Scale bar = 1 mm. (c) Cells in the cell construct are tightly
647 packed. Scale bar = 100 μ m. (d) However, cell construct cannot be formed in oil-water system.
648 (e, f) Only cell clumps are observed under inverted light microscope. Scale bars = 1 mm for (e)
649 and 100 μ m for (f).

650 **Figure SI-S3.** Result of cell construct formation experiment in PEG/sodium citrate polymer-
651 salt system. (a) Cell construct cannot be formed in polymer-salt system with all concentration
652 combination of PEG and sodium citrate. (b) MTS cell viability assay of porcine corneal
653 endothelial cell incubated in sodium citrate for 3 hours. ($n=5$, **** $p<0.0001$, one-way
654 ANOVA followed with Dunnett's test)

655

656 **Acknowledgement**

657 Funding/Support: Ho Cheung SHUM acknowledges support from the Croucher Senior
658 Research Fellowship, NSFC Excellent Young Scientists Fund (Hong Kong and Macau)
659 (21922816) as well as Research Grants Council (RGC) of Hong Kong through the NSFC/RGC
660 Joint Research Scheme (N_HKU718/19) and the General Research Fund (17305518,
661 17306820 and 17304017).

662 Yau Kei CHAN acknowledges support from both the Seed Funding for Basic Research and the
663 Startup Fund, the University of Hong Kong.

664

665 Financial Disclosures: The following authors have no relevant financial disclosures: Lap Tak
666 HUNG, Stephanie Hiu Ling POON, Wing Huen YAN, Rebecca LACE, Liangyu ZHOU,
667 Jasper Ka Wai WONG, Rachel L WILLIAMS, Kendrick Co SHIH, Ho Cheung SHUM, Yau
668 Kei CHAN

669

670 Conflict of interest: The following authors have no conflict of interest: Lap Tak HUNG,
671 Stephanie Hiu Ling POON, Wing Huen YAN, Rebecca LACE, Liangyu ZHOU, Jasper Ka
672 Wai WONG, Rachel L WILLIAMS, Kendrick Co SHIH, Ho Cheung SHUM, Yau Kei
673 CHAN

674

675 Author Contributions: All authors attest that they meet the current ICMJE criteria for
676 authorship. LTH, SHLP, WHY, RL, LZ, JKWW, RLW, KCS, HCS, YKC were involved in
677 study design, data collection, data analysis, manuscript writing and editing.

678

679 Data availability statement: Data can be made available upon reasonable request from the
680 corresponding author.

681

682 **Reference**

683

- 684 1. Mao, Z.; Fan, B.; Wang, X.; Huang, X.; Guan, J.; Sun, Z.; Xu, B.; Yang, M.; Chen, Z.; Jiang,
685 D.; Yu, J., A Systematic Review of Tissue Engineering Scaffold in Tendon Bone Healing in vivo. *Front*
686 *Bioeng Biotechnol* **2021**, *9*, 621483.
- 687 2. Yi, S.; Xu, L.; Gu, X., Scaffolds for peripheral nerve repair and reconstruction. *Exp Neurol*
688 **2019**, *319*, 112761.
- 689 3. Anderson, J. M.; Rodriguez, A.; Chang, D. T., Foreign body reaction to biomaterials. *Seminars*
690 *in Immunology* **2008**, *20* (2), 86-100.
- 691 4. Yang, J.; Yamato, M.; Kohno, C.; Nishimoto, A.; Sekine, H.; Fukai, F.; Okano, T., Cell sheet
692 engineering: Recreating tissues without biodegradable scaffolds. *Biomaterials* **2005**, *26* (33), 6415-
693 6422.
- 694 5. Matsuda, N.; Shimizu, T.; Yamato, M.; Okano, T., Tissue Engineering Based on Cell Sheet
695 Technology. *Advanced Materials* **2007**, *19* (20), 3089-3099.
- 696 6. Yamato, M.; Okano, T., Cell sheet engineering. *Materials Today* **2004**, *7* (5), 42-47.
- 697 7. Owaki, T.; Shimizu, T.; Yamato, M.; Okano, T., Cell sheet engineering for regenerative
698 medicine: Current challenges and strategies. **2014**, *9* (7), 904-914.
- 699 8. Ovsianikov, A.; Khademhosseini, A.; Mironov, V., The synergy of scaffold-based and scaffold-
700 free tissue engineering strategies. *Trends in biotechnology* **2018**, *36* (4), 348-357.
- 701 9. Whitcher, J. P.; Srinivasan, M.; Upadhyay, M. P., Corneal blindness: a global perspective.
702 *Bulletin of the World Health Organization* **2001**, *79* (3), 214-221.
- 703 10. Waring, G. O.; Bourne, W. M.; Edelhauser, H. F.; Kenyon, K. R., The Corneal Endothelium:
704 Normal and Pathologic Structure and Function. *Ophthalmology* **1982**, *89* (6), 531-590.
- 705 11. Joyce, N. C.; Harris, D. L.; Mello, D. M., Mechanisms of Mitotic Inhibition in Corneal
706 Endothelium: Contact Inhibition and TGF- β 2. *Investigative Ophthalmology & Visual Science* **2002**, *43*
707 (7), 2152-2159.
- 708 12. Van den Bogerd, B.; Dhubghaill, S. N.; Koppen, C.; Tassignon, M.-J.; Zakaria, N., A review
709 of the evidence for in vivo corneal endothelial regeneration. *Survey of Ophthalmology* **2018**, *63* (2),
710 149-165.
- 711 13. Anshu, A.; Price, M. O.; Price, F. W., Risk of Corneal Transplant Rejection Significantly
712 Reduced with Descemet's Membrane Endothelial Keratoplasty. *Ophthalmology* **2012**, *119* (3), 536-
713 540.
- 714 14. Joyce, N. C., Proliferative capacity of corneal endothelial cells. *Exp Eye Res* **2012**, *95* (1), 16-
715 23.
- 716 15. Mimura, T.; Yamagami, S.; Amano, S., Corneal endothelial regeneration and tissue
717 engineering. *Prog Retin Eye Res* **2013**, *35*, 1-17.
- 718 16. Ong, J. A.; Auvinet, E.; Forget, K. J.; Lagali, N.; Fagerholm, P.; Griffith, M.; Meunier, J.;
719 Brunette, I., 3D Corneal Shape After Implantation of a Biosynthetic Corneal Stromal Substitute.
720 *Investigative Ophthalmology & Visual Science* **2016**, *57* (6), 2355-2365.
- 721 17. Ong, H. S.; Ang, M.; Mehta, J., Evolution of therapies for the corneal endothelium: past,
722 present and future approaches. *Br J Ophthalmol* **2021**, *105* (4), 454-467.
- 723 18. Nishida, K.; Yamato, M.; Hayashida, Y.; Watanabe, K.; Maeda, N.; Watanabe, H.;
724 Yamamoto, K.; Nagai, S.; Kikuchi, A.; Tano, Y.; Okano, T., Functional bioengineered corneal
725 epithelial sheet grafts from corneal stem cells expanded ex vivo on a temperature-responsive cell
726 culture surface. *Transplantation* **2004**, *77* (3), 379-85.
- 727 19. Sridhar, M. S., Anatomy of cornea and ocular surface. *Indian J Ophthalmol* **2018**, *66* (2), 190-
728 194.
- 729 20. Mahdavi, S. S.; Abdekhodaie, M. J.; Mashayekhan, S.; Baradaran-Rafii, A.; Djalilian, A. R.,
730 Bioengineering Approaches for Corneal Regenerative Medicine. *Tissue Engineering and Regenerative*
731 *Medicine* **2020**, *17* (5), 567-593.

- 732 21. Melles, G. R.; San Ong, T.; Ververs, B.; van der Wees, J., Descemet membrane endothelial
733 keratoplasty (DMEK). *Cornea* **2006**, *25* (8), 987-990.
- 734 22. Raimondi, R.; Zollet, P.; De Rosa, F. P.; Tsoutsanis, P.; Stravalaci, M.; Paulis, M.; Inforzato,
735 A.; Romano, M. R., Where Are We with RPE Replacement Therapy? A Translational Review from the
736 Ophthalmologist Perspective. *International Journal of Molecular Sciences* **2022**, *23* (2), 682.
- 737 23. Ito, A.; Ino, K.; Kobayashi, T.; Honda, H., The effect of RGD peptide-conjugated magnetite
738 cationic liposomes on cell growth and cell sheet harvesting. *Biomaterials* **2005**, *26* (31), 6185-6193.
- 739 24. Ito, A.; Hayashida, M.; Honda, H.; Hata, K.; Kagami, H.; Ueda, M.; Kobayashi, T.,
740 Construction and harvest of multilayered keratinocyte sheets using magnetite nanoparticles and
741 magnetic force. *Tissue Eng* **2004**, *10* (5-6), 873-80.
- 742 25. Ito, A.; Hibino, E.; Kobayashi, C.; Terasaki, H.; Kagami, H.; Ueda, M.; Kobayashi, T.; Honda,
743 H., Construction and delivery of tissue-engineered human retinal pigment epithelial cell sheets, using
744 magnetite nanoparticles and magnetic force. *Tissue Eng* **2005**, *11* (3-4), 489-96.
- 745 26. Shimizu, K.; Ito, A.; Lee, J.-K.; Yoshida, T.; Miwa, K.; Ishiguro, H.; Numaguchi, Y.;
746 Murohara, T.; Kodama, I.; Honda, H., Construction of multi-layered cardiomyocyte sheets using
747 magnetite nanoparticles and magnetic force. **2007**, *96* (4), 803-809.
- 748 27. Ishii, M.; Shibata, R.; Numaguchi, Y.; Kito, T.; Suzuki, H.; Shimizu, K.; Ito, A.; Honda, H.;
749 Murohara, T., Enhanced angiogenesis by transplantation of mesenchymal stem cell sheet created by
750 a novel magnetic tissue engineering method. *Arterioscler Thromb Vasc Biol* **2011**, *31* (10), 2210-5.
- 751 28. Guillaume-Gentil, O.; Akiyama, Y.; Schuler, M.; Tang, C.; Textor, M.; Yamato, M.; Okano,
752 T.; Vörös, J., Polyelectrolyte Coatings with a Potential for Electronic Control and Cell Sheet
753 Engineering. **2008**, *20* (3), 560-565.
- 754 29. Guillaume-Gentil, O.; Semenov, O. V.; Zisch, A. H.; Zimmermann, R.; Vörös, J.; Ehrbar, M.,
755 pH-controlled recovery of placenta-derived mesenchymal stem cell sheets. *Biomaterials* **2011**, *32*
756 (19), 4376-4384.
- 757 30. Yamada, N.; Okano, T.; Sakai, H.; Karikusa, F.; Sawasaki, Y.; Sakurai, Y., Thermo-responsive
758 polymeric surfaces; control of attachment and detachment of cultured cells. **1990**, *11* (11), 571-576.
- 759 31. Yaji, N.; Yamato, M.; Yang, J.; Okano, T.; Hori, S., Transplantation of tissue-engineered
760 retinal pigment epithelial cell sheets in a rabbit model. *Biomaterials* **2009**, *30* (5), 797-803.
- 761 32. Miyahara, Y.; Nagaya, N.; Kataoka, M.; Yanagawa, B.; Tanaka, K.; Hao, H.; Ishino, K.;
762 Ishida, H.; Shimizu, T.; Kangawa, K.; Sano, S.; Okano, T.; Kitamura, S.; Mori, H., Monolayered
763 mesenchymal stem cells repair scarred myocardium after myocardial infarction. *Nat Med* **2006**, *12*
764 (4), 459-65.
- 765 33. Matsuura, K.; Wada, M.; Konishi, K.; Sato, M.; Iwamoto, U.; Sato, Y.; Tachibana, A.;
766 Kikuchi, T.; Iwamiya, T.; Shimizu, T.; Yamashita, J. K.; Yamato, M.; Hagiwara, N.; Okano, T.,
767 Fabrication of Mouse Embryonic Stem Cell-Derived Layered Cardiac Cell Sheets Using a Bioreactor
768 Culture System. *PLOS ONE* **2012**, *7* (12), e52176.
- 769 34. Haraguchi, Y.; Matsuura, K.; Shimizu, T.; Yamato, M.; Okano, T., Simple suspension culture
770 system of human iPS cells maintaining their pluripotency for cardiac cell sheet engineering. *J Tissue*
771 *Eng Regen Med* **2015**, *9* (12), 1363-75.
- 772 35. Akiyama, Y.; Kikuchi, A.; Yamato, M.; Okano, T., Ultrathin Poly(N-isopropylacrylamide)
773 Grafted Layer on Polystyrene Surfaces for Cell Adhesion/Detachment Control. *Langmuir* **2004**, *20*
774 (13), 5506-5511.
- 775 36. Nagase, K.; Yamato, M.; Kanazawa, H.; Okano, T., Poly(N-isopropylacrylamide)-based
776 thermoresponsive surfaces provide new types of biomedical applications. *Biomaterials* **2018**, *153*,
777 27-48.
- 778 37. Huang, D.-M.; Chung, T.-H.; Hung, Y.; Lu, F.; Wu, S.-H.; Mou, C.-Y.; Yao, M.; Chen, Y.-C.,
779 Internalization of mesoporous silica nanoparticles induces transient but not sufficient osteogenic
780 signals in human mesenchymal stem cells. *Toxicology and Applied Pharmacology* **2008**, *231* (2), 208-
781 215.

782 38. Martínez, J. S.; Keller, T. C. S., 3rd; Schlenoff, J. B., Cytotoxicity of free versus multilayered
783 polyelectrolytes. *Biomacromolecules* **2011**, *12* (11), 4063-4070.

784 39. Cooperstein, M. A.; Canavan, H. E., Assessment of cytotoxicity of (N-isopropyl acrylamide)
785 and poly(N-isopropyl acrylamide)-coated surfaces. *Biointerphases* **2013**, *8* (1), 19-19.

786 40. Teixeira, A. G.; Agarwal, R.; Ko, K. R.; Grant-Burt, J.; Leung, B. M.; Frampton, J. P., Emerging
787 Biotechnology Applications of Aqueous Two-Phase Systems. *Adv. Healthc. Mater.* **2018**, *7*, e1701036.

788 41. González-Valdez, J.; Mayolo-Deloisa, K.; Rito-Palomares, M., Novel aspects and future
789 trends in the use of aqueous two-phase systems as a bioengineering tool. *Journal of Chemical*
790 *Technology & Biotechnology* **2018**, *93* (7), 1836-1844.

791 42. Chao, Y.; Shum, H. C., Emerging aqueous two-phase systems: from fundamentals of
792 interfaces to biomedical applications. *Chemical Society Reviews* **2019**.

793 43. Ma, Q.; Song, Y.; Sun, W.; Cao, J.; Yuan, H.; Wang, X.; Sun, Y.; Shum, H. C., Cell-Inspired
794 All-Aqueous Microfluidics: From Intracellular Liquid-Liquid Phase Separation toward Advanced
795 Biomaterials. *Advanced Science* **2020**, *7* (7), 1903359.

796 44. Chan, Y. K.; Yan, W. H.; Hung, L. T.; Chao, Y.; Wu, J.; Shum, H. C., All-Aqueous Thin-Film-
797 Flow-Induced Cell-Based Monolayers. *ACS Applied Materials & Interfaces* **2019**, *11* (25), 22869-
798 22877.

799 45. Han, C.; Takayama, S.; Park, J., Formation and manipulation of cell spheroids using a density
800 adjusted PEG/DEX aqueous two phase system. *Scientific reports* **2015**, *5*, 11891.

801 46. Frampton, J. P.; Leung, B. M.; Bingham, E. L.; Leshner-Perez, S. C.; Wang, J. D.; Sarhan, H. T.;
802 El-Sayed, M. E. H.; Feinberg, S. E.; Takayama, S., Rapid Self-Assembly of Macroscale Tissue
803 Constructs at Biphasic Aqueous Interfaces. *Adv. Funct. Mater.* **2015**, *25*, 1694-1699.

804 47. Araki-Sasaki, K.; Ohashi, Y.; Sasabe, T.; Hayashi, K.; Watanabe, H.; Tano, Y.; Handa, H., An
805 SV40-immortalized human corneal epithelial cell line and its characterization. *Investigative*
806 *Ophthalmology and Visual Science* **1995**, *36* (3), 614-621.

807 48. Proulx, S.; Bourget, J.-M.; Gagnon, N.; Martel, S.; Deschambeault, A.; Carrier, P.; Giasson,
808 C. J.; Auger, F. A.; Brunette, I.; Germain, L., Optimization of culture conditions for porcine corneal
809 endothelial cells. *Molecular vision* **2007**, *13*, 524-533.

810 49. Frampton, J. P.; Leung, B. M.; Bingham, E. L.; Leshner-Perez, S. C.; Wang, J. D.; Sarhan, H. T.;
811 El-Sayed, M. E. H.; Feinberg, S. E.; Takayama, S., Rapid Self-Assembly of Macroscale Tissue
812 Constructs at Biphasic Aqueous Interfaces. **2015**, *25* (11), 1694-1699.

813 50. Schneider, C. A.; Rasband, W. S.; Eliceiri, K. W., NIH Image to ImageJ: 25 years of Image
814 Analysis. *Nature Methods* **2012**, *9*, 671-675.

815 51. Hayashi, T.; Yuda, K.; Oyakawa, I.; Kato, N., Use of Brilliant Blue G in Descemet's Membrane
816 Endothelial Keratoplasty. *BioMed Research International* **2017**, *2017*, 9720389.

817 52. Terzariol, M.; Hünning, P. S.; Brambatti, G.; Albuquerque, L. d.; Neumann, C.; Pigatto, J. A.
818 T., Effects of intracameral brilliant blue on the corneal endothelium of swine: in vitro study. *Pesquisa*
819 *Veterinária Brasileira* **2016**, *36*, 775-780.

820 53. Gallagher, A. G.; Alorabi, J. A.; Wellings, D. A.; Lace, R.; Horsburgh, M. J.; Williams, R. L., A
821 Novel Peptide Hydrogel for an Antimicrobial Bandage Contact Lens. *Adv Healthc Mater* **2016**, *5* (16),
822 2013-8.

823 54. Lace, R.; Duffy, G. L.; Gallagher, A. G.; Doherty, K. G.; Maklad, O.; Wellings, D. A.; Williams,
824 R. L., Characterization of Tunable Poly-epsilon-Lysine-Based Hydrogels for Corneal Tissue
825 Engineering. *Macromol Biosci* **2021**, *21* (7), e2100036.

826 55. Kennedy, S.; Lace, R.; Carserides, C.; Gallagher, A. G.; Wellings, D. A.; Williams, R. L.; Levis,
827 H. J., Poly-epsilon-lysine based hydrogels as synthetic substrates for the expansion of corneal
828 endothelial cells for transplantation. *J Mater Sci Mater Med* **2019**, *30* (9), 102.

829 56. Gasperino, D.; Meng, L.; Norris, D. J.; Derby, J. J., The role of fluid flow and convective
830 steering during the assembly of colloidal crystals. *Journal of Crystal Growth* **2008**, *310* (1), 131-139.

831 57. Chen, M.; Cölfen, H.; Polarz, S., Centrifugal Field-Induced Colloidal Assembly: From Chaos to
832 Order. *ACS Nano* **2015**, *9* (7), 6944-6950.

833 58. Qi, X.; Li, M.; Kuang, Y.; Wang, C.; Cai, Z.; Zhang, J.; You, S.; Yin, M.; Wan, P.; Luo, L.; Sun,
834 X., Controllable Assembly and Separation of Colloidal Nanoparticles through a One-Tube Synthesis
835 Based on Density Gradient Centrifugation. *Chemistry – A European Journal* **2015**, *21* (19), 7211-7216.

836 59. Hua, C.; Xu, H.; Zhang, P.; Chen, X.; Lu, Y.; Gan, Y.; Zhao, J.; Li, Y., Process optimization and
837 optical properties of colloidal self-assembly via refrigerated centrifugation. *Colloid and Polymer*
838 *Science* **2017**, *295* (9), 1655-1662.

839 60. Luh, E. H.; Shackford, S. R.; Shatos, M. A.; Pietropaoli, J. A., The Effects of Hyperosmolarity
840 on the Viability and Function of Endothelial Cells. *Journal of Surgical Research* **1996**, *60* (1), 122-128.

841 61. Edelhauser, H. F.; Hanneken, A. M.; Pederson, H. J.; Van Horn, D. L., Osmotic Tolerance of
842 Rabbit and Human Corneal Endothelium. *Archives of Ophthalmology* **1981**, *99* (7), 1281-1287.

843 62. Noske, W.; Fromm, M.; Levarlet, B.; Kreusel, K. M.; Hirsch, M., Tight junctions of the human
844 corneal endothelium: morphological and electrophysiological features. *Ger J Ophthalmol* **1994**, *3* (4-
845 5), 253-257.

846 63. Therien, A. G.; Blostein, R., Mechanisms of sodium pump regulation. *American Journal of*
847 *Physiology-Cell Physiology* **2000**, *279* (3), C541-C566.

848 64. Cornea Donor Study Investigator, G.; Lass, J. H.; Gal, R. L.; Dontchev, M.; Beck, R. W.;
849 Kollman, C.; Dunn, S. P.; Heck, E.; Holland, E. J.; Mannis, M. J.; Montoya, M. M.; Schultze, R. L.;
850 Stulting, R. D.; Sugar, A.; Sugar, J.; Tennant, B.; Verdier, D. D., Donor age and corneal endothelial
851 cell loss 5 years after successful corneal transplantation. Specular microscopy ancillary study results.
852 *Ophthalmology* **2008**, *115* (4), 627-632.e8.

853 65. Melles, G. R. J.; Ong, T. S.; Ververs, B.; van der Wees, J., Descemet Membrane Endothelial
854 Keratoplasty (DMEK). *Cornea* **2006**, *25* (8).

855 66. Kobayashi, T.; Kan, K.; Nishida, K.; Yamato, M.; Okano, T., Corneal regeneration by
856 transplantation of corneal epithelial cell sheets fabricated with automated cell culture system in
857 rabbit model. *Biomaterials* **2013**, *34* (36), 9010-9017.

858 67. Gupta, S., Gupta, P., Sayegh, R. Healing a Persistent Corneal Epithelial Defect 2014, p. 33 -
859 35. (accessed 2020).

860 68. Baradaran-Rafii, A.; Eslani, M.; Haq, Z.; Shirzadeh, E.; Huvard, M. J.; Djalilian, A. R., Current
861 and Upcoming Therapies for Ocular Surface Chemical Injuries. *Ocul Surf* **2017**, *15* (1), 48-64.

862 69. Rahman, I.; Carley, F.; Hillarby, C.; Brahma, A.; Tullo, A. B., Penetrating keratoplasty:
863 indications, outcomes, and complications. *Eye (Lond)* **2009**, *23* (6), 1288-94.

864 70. Groves, R. W., & Schmidt-Lucke, J. A., Recombinant human GM-CSF in the treatment of
865 poorly healing wounds. *Advances in skin & wound care* **2000**, *13*, 107.

866 71. Rho, C. R.; Park, M.-y.; Kang, S., Effects of granulocyte-macrophage colony-stimulating (GM-
867 CSF) factor on corneal epithelial cells in corneal wound healing model. *PloS one* **2015**, *10* (9),
868 e0138020.

869 72. Boisjoly, H. M.; Laplante, C.; Bernatchez, S. F.; Salesse, C.; Giasson, M.; Joly, M.-C., Effects
870 of EGF, IL-1 and their combination on in vitro corneal epithelial wound closure and cell chemotaxis.
871 *Experimental eye research* **1993**, *57* (3), 293-300.

872 73. Bird, T.; Saklatvala, J., IL-1 and TNF transmodulate epidermal growth factor receptors by a
873 protein kinase C-independent mechanism. *The Journal of Immunology* **1989**, *142* (1), 126-133.

874 74. Wilson, S. E.; He, Y. G.; Weng, J.; Li, Q.; McDowall, A. W.; Vital, M.; Chwang, E. L., Epithelial
875 injury induces keratocyte apoptosis: hypothesized role for the interleukin-1 system in the
876 modulation of corneal tissue organization and wound healing. *Exp Eye Res* **1996**, *62* (4), 325-7.

877 75. Saika, S., Yin and yang in cytokine regulation of corneal wound healing: roles of TNF- α .
878 *Cornea* **2007**, *26*, S70-S74.

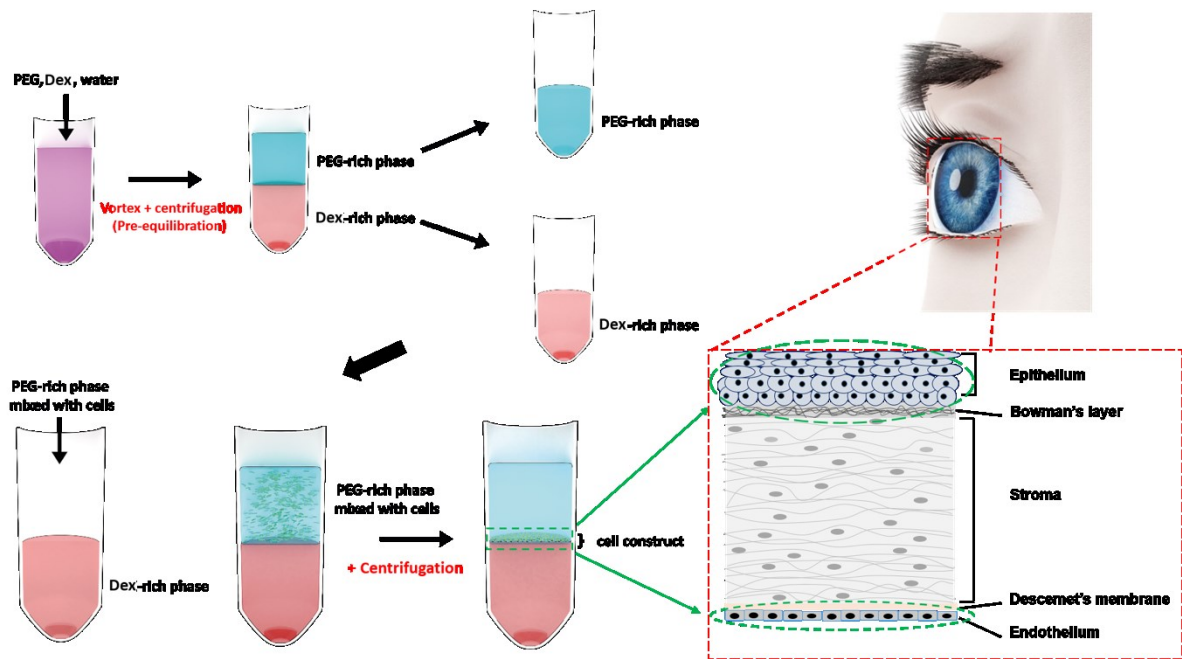
879 76. Wang, X.; Zhang, S.; Dong, M.; Li, Y.; Zhou, Q.; Yang, L., The proinflammatory cytokines IL-
880 1 β and TNF- α modulate corneal epithelial wound healing through p16Ink4a suppressing STAT3
881 activity. *Journal of Cellular Physiology* **2020**, *235* (12), 10081-10093.

- 882 77. Geremicca, W.; Fonte, C.; Vecchio, S., Blood components for topical use in tissue
883 regeneration: evaluation of corneal lesions treated with platelet lysate and considerations on repair
884 mechanisms. *Blood Transfusion* **2010**, *8* (2), 107.
- 885 78. Arranz-Valsero, I.; Soriano-Romaní, L.; García-Posadas, L.; López-García, A.; Diebold, Y., IL-6
886 as a corneal wound healing mediator in an in vitro scratch assay. *Experimental eye research* **2014**,
887 *125*, 183-192.
- 888 79. Hashimoto, S.; Yoda, M.; Yamada, M.; Yanai, N.; Kawashima, T.; Motoyoshi, K.,
889 Macrophage colony-stimulating factor induces interleukin-8 production in human monocytes. *Exp*
890 *Hematol* **1996**, *24* (2), 123-8.
- 891 80. Shah, R. K.; Shum, H. C.; Rowat, A. C.; Lee, D.; Agresti, J. J.; Utada, A. S.; Chu, L.-Y.; Kim, J.-
892 W.; Fernandez-Nieves, A.; Martinez, C. J.; Weitz, D. A., Designer emulsions using microfluidics.
893 *Materials Today* **2008**, *11* (4), 18-27.
- 894 81. Kim, J. H.; Jeon, T. Y.; Choi, T. M.; Shim, T. S.; Kim, S.-H.; Yang, S.-M., Droplet Microfluidics
895 for Producing Functional Microparticles. *Langmuir* **2014**, *30* (6), 1473-1488.
- 896 82. Sah, H., Protein behavior at the water/methylene chloride interface. *J Pharm Sci* **1999**, *88*
897 (12), 1320-5.
- 898 83. MCCLEMENTS, D. J.; DECKER, E. A., Lipid Oxidation in Oil-in-Water Emulsions: Impact of
899 Molecular Environment on Chemical Reactions in Heterogeneous Food Systems. **2000**, *65* (8), 1270-
900 1282.
- 901 84. Silvério, S. C.; Wegrzyn, A.; Lladosa, E.; Rodríguez, O.; Macedo, E. A., Effect of Aqueous
902 Two-Phase System Constituents in Different Poly(ethylene glycol)–Salt Phase Diagrams. *Journal of*
903 *Chemical & Engineering Data* **2012**, *57* (4), 1203-1208.
- 904 85. Kubota, A.; Nishida, K.; Yamato, M.; Yang, J.; Kikuchi, A.; Okano, T.; Tano, Y.,
905 Transplantable retinal pigment epithelial cell sheets for tissue engineering. *Biomaterials* **2006**, *27*
906 (19), 3639-3644.
- 907 86. Ao, J.; Wood, J. P.; Chidlow, G.; Gillies, M. C.; Casson, R. J., Retinal pigment epithelium in
908 the pathogenesis of age-related macular degeneration and photobiomodulation as a potential
909 therapy? *Clin Exp Ophthalmol* **2018**, *46* (6), 670-686.
- 910 87. Bonilha, V. L., Age and disease-related structural changes in the retinal pigment epithelium.
911 *Clin Ophthalmol* **2008**, *2* (2), 413-424.

912

913

914 Table of Contents graphic



915

916

917